SRTTU

JCARME
ISSN: 2228-7922
Journal of Computational and Applied Research in Mechanical Engineering
Vol. 8, No. 2, pp. 153-164
jcarme.sru.ac.ir

Experimental and numerical investigation of bottom outlet hydraulic model

M. Moghimi*, M. Kalantar and E. Molavi

School of Mechanical Engineering, Iran University of Science and Technology (IUST), Tehran, Iran

Article info:

Received: 15/06/2016
Accepted: 26/08/2018
Online: 29/08/2018

Keywords:
Numerical simulation,
Dam bottom outlet,
Volume of fluid,
Ventilation.

Abstract

Using experimental models along with conducting numerical analysis have been widely used in performance recognition and optimization of hydraulic equipment. Numerical modeling has lower cost rather than experimental one; however practical tests are commonly used because of the hydraulic structure importance especially in dams. Meanwhile, numerical methods could be used for the future designs by validating numerical models. In this paper, the volume of the fluid method is employed to simulate the free surface flow at the dam bottom outlet form a bell mouth section up to the downstream channel. Since the flow through the gates is turbulent, the standard k-ε, Reynolds Stress Model, RSM, and turbulence models are used, and the results are compared. The discharge coefficient and the ventilated air velocity through the vents are computed numerically and compared with the experimental data. Comparison between the experimental data and numerical simulation results shows good compatibility, especially in the Reynolds Stress and turbulence models rather than the k-ε turbulence model. The results show that the maximum error percentage in the simulation of the discharge coefficient and the ventilated air velocity is 9% and 3%, respectively.

Nomenclature

Q	Flow rate
A	Area
A_0	Maximum area of the exit cross section
g	Gravitational acceleration
H	Head behind the valve
H_e	Head drop before the minimum height section
Z_c	Height for the minimum section
C_d	Discharge coefficient
H_{max},	Maximum head
H_{normal},	Normal head
H_{min}	Minimum head
K	Turbulent kinetic energy
ε	Turbulent dissipation energy
μ	Viscosity
ρ	Density

1. Introduction

Through technology promotion and the needs for developing water resources, designing and manufacturing huge hydro-structures have significantly become important. A great deal of time and expenses have been spent to build giant hydraulic structures. Furthermore, according to the fact that experimentation is still the only confident way to evaluate the performance of

*Corresponding author
email address: moghimi@iust.ac.ir

these kinds of structures, the scientists and designers have got the idea to clarify the obscure aspects of structure designing by means of manufacturing physical models and simulating the flow through conducting various experiments. In this procedure, necessary frugality could be achieved and the errors and defects of the project could be solved. By a single rise in the height of water in hydro-structures, serious problems thread the lower evacuating ducts which have vital roles in regulating the evacuation of the dams' reservoirs. In this design, the exhaust ducts that are controlled by sliding valves due to their fewer vibrations are exposed to high speed flows in the valve downstream which could lead to extreme pressure drops. If they become lower than the satirized vapor pressure, they could cause damages due to destructive phenomena such as cavitation or the structure vibrations.

The problems raised by cavitation and vibrations on the valves related to the evacuations ducts are produced due to the reasons such as pressure drop in the water flow and weak aeration in low-pressure places. According to the fact, the flow on the slot and beneath the valves of such evacuation ducts is mostly accompanied by separation, precise design of the geometry of the valve slot area, and sufficient aeration to the flow. These are the most important parameters of designing among which sufficient aeration could, on the one hand, remove the vacancy produced in the downstream tunnel and prevent cavitation and, on the other hand, reduce the valve's vibrations. Accordingly, it is necessary to investigate the parameters and also their influence on intensifying or preventing cavitation and vibrations by means of empirical processes and required tests. After ensuring the correct performance of the evacuation, duct and its valves are set up to build the main structure.

Air entrainment into the pipes was first presented by Kalinske and Robertson in 1943 [1]. They investigated the origin of hydraulic jump and how it affects the air entrainment into the pipes. In 1976, Sharma divided the aerated flow after the valve into three categories of free surface flow, spraying flow and hydraulic jump [2]. In 1997, Speerli and Volkart [3] studied the amount of air required in a rectangular tunnel and eventually made a relation between the air vent evacuation and other various parameters. Kenn and Garrod, in 1981, studied the damages produced by cavitation on the tunnel of the investigated dam [4]. Furthermore, air concentration profiles in a free surface flow in the gate downstream have also been measured by Hager in 2000 [5].

In 2008, Safavi et al. [6] experimentally investigated the effects of parameters including gate opening, vent diameter and tunnel dimensions on the vent discharge and air supplied from the tunnel outlet in a circular tunnel. They came to the conclusion that relative flow depth (i.e., the ratio of flow depth to the tunnel diameter) and the vent opening have significant influences on the air supplied from the tunnel outlet other than FRC. Experimental modeling as well as numerical simulation of Aswan Dam, Egypt, were used by Dargahi [7] to obtain the discharge coefficient of a moving gate valve in the bottom outlet. Numerical simulation by RNG turbulence model showed good compatibility.

Yazdi in 2010 simulated aeration in high speed flows inside a tunnel in order to prevent the destructive effects of cavitation [8]. This study was performed for rectangular and circular sections, and volume of fluid (VOF) model was employed for the purpose of modeling the free surface flow. Kolachian et al. [9] in 2012 used the VOF model to simulate the water surface profile, mean velocity, static pressure, and cavitation index before and after aeration. Their results showed the relative capability of numerical models in flow simulation in the bottom outlet conduit of a dam and improved flow conditions after aeration. In 2015, Kiczko et al. [10] used a potential field as a numerical model to simulate flow under a sluice gate. Comparison between experimental data and their results showed a satisfactory agreement. However, they reported overestimation of the Reynolds averged Navier Stokes (RANS) model results in terms of energy losses. To evaluate the capability of the computational fluid dynamics (CFD) on modeling spillway flow, Kumcu, [11] in 2016 compared the results obtained from physical modeling by CFD simulation results which showed reasonably good agreement

between the physical and numerical models in flow characteristics.
In this research, the bottom channel model is made by Plexiglas in the scale of 1:18 containing the discharge valves which are of sliding types. This model is tested as well, by setting various flow rates corresponding to real conditions, and the tests are carried out by measuring critical flow parameters (velocity and pressure). The research is followed up by numerical investigations accompanied by k-ε and Reynolds Stress Models (RSM) for numerically analyzing the two-phase flow inside the bottom evacuation valve of a dam. Regarding both models, the results obtained from the numerical results, are compared to the empirical ones. Validation is carried out and a more suitable turbulence model is introduced. Finally, the simulation results for the vent discharge velocity and the rate of air supply from the tunnel outlet for the various openings are reported.

2. Effective parameters

Despite the fact that there are exact answers for the fluid statics and many other laminar flow problems, solving the general equations in turbulent flows by using the most advanced computers has only been led to an acceptable approximation of answers which require comparison and confirmation to experimental data. The dimensional analysis similarity could provide the experimental models with implementation together with analysis and interpretation of the data. Therefore, making dimensionless parameters seems critical.
Generally, the mass flow rate passing through the lower valves of the dam is a function of geometrical and physical parameters.

$$Q = F(A, A_0, g, H, \mu, \rho, H_e, Z_c) \quad (1)$$

In Eq. (1), ρ is the fluid density, μ is the dynamic viscosity, *H* is the head behind the valve, g is the gravitational acceleration, A_0 is the maximum area of the exit cross section of the valve, A is the exit cross-section of the valve, H_e is the head drop before the minimum height section, and z_c is the height for the minimum section. According to the extracted parameters and due to the π-Buckingham theorem, the analysis would lead to the following four dimensionless numbers.

$$G\left(\frac{\rho}{\mu}\frac{Q}{H}, \frac{Q}{A\sqrt{2g(H-H_e-z_c-H_c)}}, \frac{A}{A_0}, \frac{A_0}{H^2}\right) = 0 \quad (2)$$

In Eq. (2), $\frac{\rho}{\mu}\frac{Q}{H}$ is the Reynolds number, $\frac{A}{A_0}$ is the percentage of the valve opening, $\frac{A_0}{H^2}$ is the valve characteristic, and H_c is the head due to the fluid velocity in the section of the minimum height. The other parameter is of significant importance in this study which includes the discharge coefficient defined as below:

$$C_d = \frac{Q}{A\sqrt{2gH}} \quad (3)$$

2. 1. Effective dimensionless parameters

The maximum, normal and minimum heads for the Darian dam are as follows:

$$\begin{aligned} H_{\max} &= 141.5\ m \\ H_{normal} &= 121.5\ m \\ H_{\min} &= 41.5\ m \end{aligned} \quad (4)$$

Due to the upstream DWG's of the desired region, the pressure drop is calculated which is about 1.5 m H_2O. Accordingly, the values for the heads are modified as below, and the rest of the calculations are done based on the modification:

$$\begin{aligned} H_{\max} &= 140\ m \\ H_{\text{normal}} &= 120\ m \\ H_{\min} &= 40\ m \end{aligned} \quad (5)$$

According to the Darian dam's documents, A_0 and the maximum flow rate are 5.72 m^2 and 250 m^3/sec, respectively. It is obvious that A is equal to A_0 in this flow rate. Therefore, the following dimensionless numbers are obtained based on the values associated with the original prototype for an opening of 100% and scale of 1:18.

$$\frac{A}{A_0} = 1 \quad , \quad A_0 = 5.72\,m^2$$

$$\frac{Q}{A\sqrt{2gH}} = \quad 0.8295$$

$$\frac{A_0}{H^2} = 2.86\times10^{-4}$$
$$\frac{\rho}{\mu}\frac{Q}{H} = 1.78\times10^{6} \quad (6)$$

Not only the order for A_0/H^2 is much smaller than that of the others, but also it has no considerable variations inside the range of operational condition. Hence it has no significant effect on the valve performance. In addition, inside a wide range of flow rate variations, high enough Reynolds numbers, it remains high with limited variance. It is true that where the gate valve opening is not so small the separate hydraulic modeling is required. It means, in the opening gate valve lower than 10%, it is essential to investigate the effects of Reynolds number as well. On the other hand, if the gate valve opening is more than about 10%, Reynolds number has no significant influence on other parameters. As explained above, two main dimensionless parameters should be considered in the analysis which are $Q/A\sqrt{2gH}$ and A/A_0. Thereby Eq. (2) should be replaced with the following formula:

$$\frac{Q}{A\sqrt{2gH}} = \Phi\left(\frac{A}{A_0}\right) \quad (7)$$

3. Hydraulic test setup and the test procedure

In order to study the hydraulic behavior of the Darian dam bottom outlet, the upstream channel is made of carbon steel pipe with a transition according to the full-scale dimensions in the scale of 1:18.

To study the behavior of the water jet, the tunnel should be transparent which are made by Plexiglas up to the end of the downstream tunnel. This region is scaled geometrically based on the Darian DWGs. In order to have a closed loop, a pump with a suction line of 8" pipe is used to circulate the water in the channels. The flow rate of the pump is controlled by means of a by-pass with a valve on a 6" pipe. There is a storage tank with a volume of 4 m^3. So in this loop, water is pumped from the storage tank and flows to the upstream and downstream channel; finally goes back to a storage tank. Fig. 1 shows a schematic of the test loop. To check the hydraulic similarity between the real scale and the model scale, a reference point in the model test should be assessed. The pressure in the reference point (after the bell mouth section) is supposed to be 7.86 m H_2O when the gate valve is closed according to the similarity laws.

Thus the flow rate and the static pressure in the model reference point are recorded which should be 7.86 m H_2O in total pressure scale during the test for the maximum head in the real scale dam. It means that if the gate valve is opened, i.e. from 20% to 30%, the bypass valve near the pump should be adjusted to maintain the total pressure at the reference point the same as in the 20% opening. Moreover, there is a time (about 20 s) needed to reach the system to its steady state condition. A data acquisition system is used which consists of the 64 pressure transducers in the range of 10 kPa, 50 kPa and 100 kPa in absolute and differential types. Also, the flow rate is recorded with Endress-Hauser flow meter Promag 50 at the upstream of the test loop, Fig. 2.

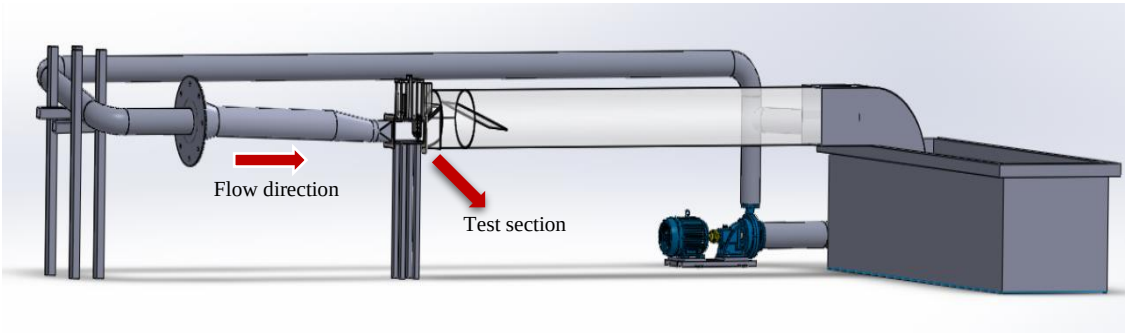

Fig. 1. Schematic of the test loop.

The pressure data and the flow rate are recorded with 1 K samples per second to study any transient event in the channels. The gathered data are processed off-line in a MATLAB code. In addition, each test should be repeated at least three times to ensure the repeatability of the data. These set of test should be performed for different gate valve openings. These pressure transducers are installed in different locations of the channels, especially in the vicinity of the emergency and service gates, as depicted in Fig. 3.

(a) (b)

Fig. 2. (a) pressure box, (b) magnetic flow meter.

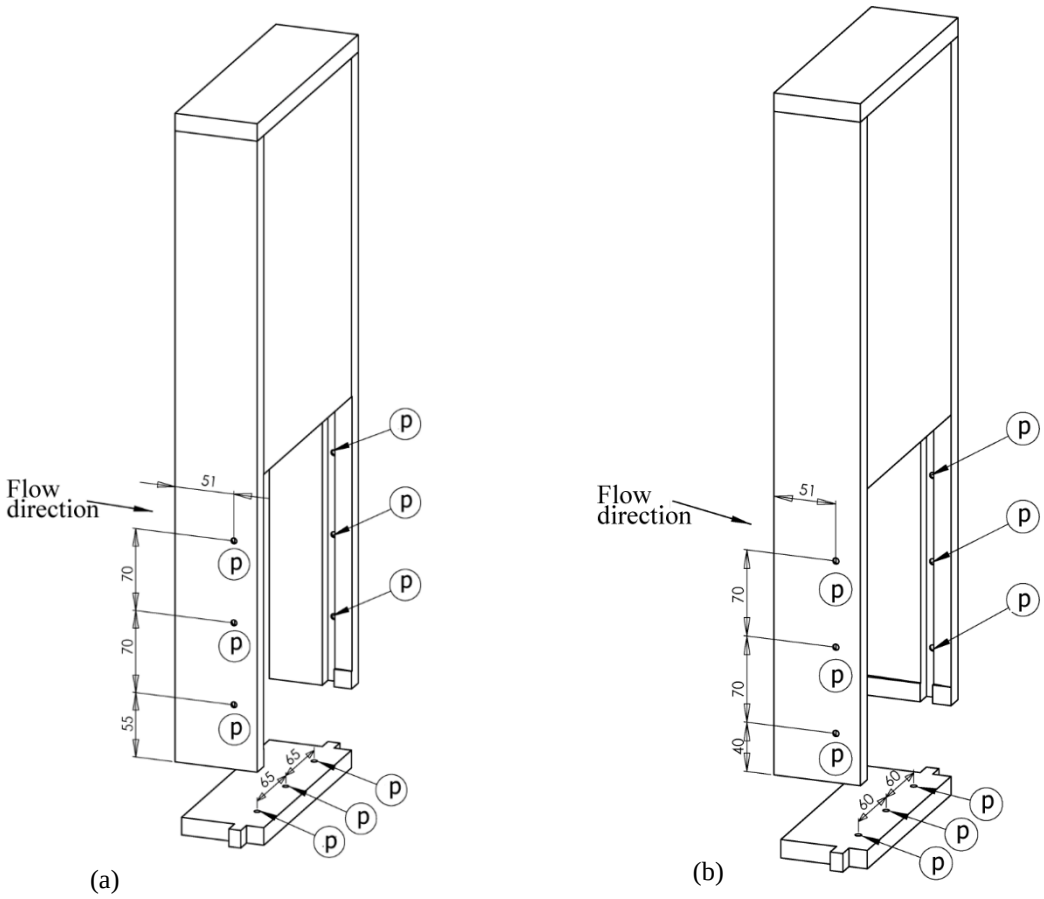

(a) (b)

Fig. 3. Pressure transducers locations; (a) emergency gate valve, and (b) service gate valve.

There are 64 points totally which the pressure time histories are recorded, and after some noise filtering, the data are used in the computation of different parameters such as discharge coefficient and cavitation number. All these points are connected to the pressure box embedded near the gate valves using flexible hoses with an external diameter of 4 mm as illustrated in Fig. 4. It should be noted that all data from different points in upstream and downstream channels are recorded simultaneously by Motorola pressure transducers of series MPX5010, MPX5050 and MPC5100. To record the data, a C program is developed (Hydrolab data logger, Hydrodynamics laboratory, Iran University of Science and Technology). In this program, two variables are adjusted in the calibration procedure and determined separately for each sensor in the calibration stage.

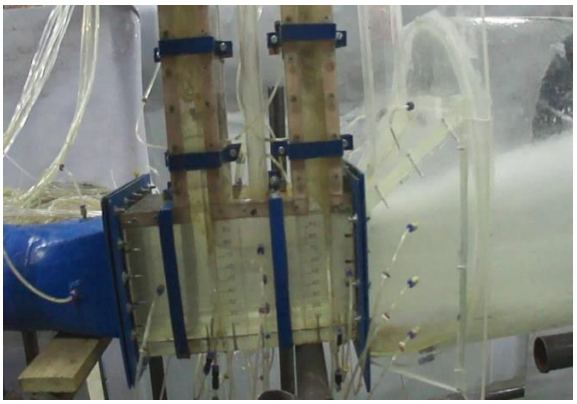

Fig. 4. Test section.

Another parameter is the air velocity in the ducts between the gates in expansion section. In this study, the service gate valve operation and the emergency gate valve are assumed to be fully open. Hence the air velocity in the duct over the expansion section is reported. To record the air velocity, a hot wire sensor (model AM-4204) is employed which is also capable of measuring the temperature. The air velocity for different service gate valve openings is demonstrated in Fig. 5 showing good compatibility in comparison with Sharma equation [2].

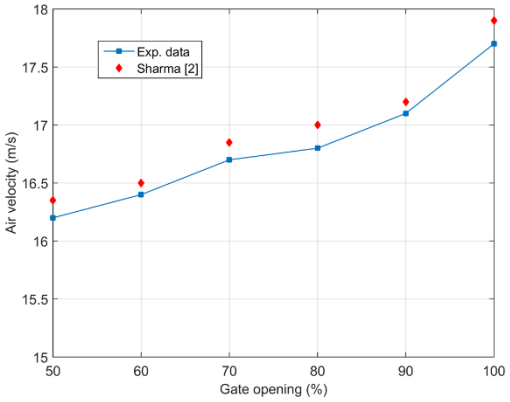

Fig. 5. Variations of the air velocity ventilation in different service gate valve openings.

4. Numerical simulation

The fundamental governing equations of the fluid flow are given by the Navier–Stokes equations in addition to the mass conservation constraint. The latter is given by the continuity equation [12].

$$\frac{\partial \rho}{\partial t} + \nabla \rho U = 0 \tag{8}$$

For an incompressible fluid, ρ is constant, and the continuity equation reduces to $\partial \rho / \partial t = 0$. Neglecting the gravity force, the momentum equation is given by:

$$\frac{\partial (\rho U)}{\partial t} + (U \nabla)(\rho U) = \nabla T + f_{st} \tag{9}$$

where $U = (u, v, w)$ is the velocity vector and f_{st} is the surface tension force. Surface tension deals with a macroscopic level based on the statistical behavior of interfaces. The total stress tensor, *T*, for a Newtonian fluid in local thermodynamic equilibrium, which is not exposed to very high temperature or pressure ranges, is defined as:

$$T = -\left(p + \frac{2}{3} \mu \nabla U \right) I + 2 \mu D \tag{10}$$

where p is the pressure, μ is the dynamic viscosity of the fluid, D is the rate of strain tensor, and I is the unit tensor. Considering the

incompressibility condition $T = -gradp + 2\nabla\mu D$, the strain rate tensor is expressed as:

$$D = \frac{1}{2}\left[\nabla U + (\nabla U)^T\right] \tag{11}$$

Hence, for an incompressible fluid:

$$2\nabla(\mu D) = \nabla(\mu\nabla D) + (\nabla D)\nabla\mu \tag{12}$$

The equations of motion are closed with the constitutive relations for the density and dynamic viscosity as:

$$\begin{aligned} \rho &= \alpha\rho_1 + (1-\alpha)\rho_2 \\ \mu &= \alpha\mu_1 + (1-\alpha)\mu_2 \end{aligned} \tag{13}$$

Here, subscripts 1 and 2 denote the different fluids. The indicator function α represents the volume fraction of fluid 1 in the computational cell:

$$\alpha(x,t) = \begin{cases} 1 & \text{for the point (x,t) inside fluid 1} \\ 0 & \text{for the point (x,t) inside fluid 2} \\ 0 < \alpha < 1 & \text{for the point (x,t) inside transitional area} \end{cases} \tag{14}$$

So it is equivalent to $\rho = (\rho_1 - \rho_2)\alpha + \rho_2$. Using the continuity equation, $d\rho/dt = 0$, yields immediately a zero material derivative $d\alpha/dt = 0$, equivalent to:

$$\frac{d\alpha}{dt} = \frac{\partial\alpha}{\partial t} + U\nabla\alpha = 0 \tag{15}$$

These values, therefore, are propagated with the fluids as a Lagrangian invariant and thus have a zero material derivative. Therefore, it completes the mathematical description of the two-fluid systems for laminar flows. The equations derived above are general and completely describe the motions of the two fluids and the interface between them. In this study, the gravitational effects are neglected, and the fluids are assumed to be incompressible. Thus, the continuity equation is expressed as:

$$\begin{aligned} \nabla U &= \frac{-1}{\rho}\frac{d}{dt}\left[\alpha(\rho_1 - \rho_2) + \rho_2\right] \\ &= \frac{-(\rho_1 - \rho_2)}{\rho}\left(\frac{d\alpha}{dt}\right) = 0 \end{aligned} \tag{16}$$

The incompressibility condition (Eq. (16)) can be used to rearrange the transport equation for α (Eq. (15)) into a conservative form suitable for finite volume discretization by adding a zero term $\alpha\nabla U$ to Eq. (15). This results in the following equation:

$$\frac{\partial\rho}{\partial t} + \nabla\rho U = 0 \tag{17}$$

The incompressibility condition (Eq. (16)) can also be used to reduce some of the terms in the stress tensor (Eq. (10)), thus simplifying the momentum equations to:

$$\begin{aligned} \frac{\partial\rho U}{\partial t} + (U\nabla)(\rho U) &= -\nabla p + \nabla(\mu\nabla U) \\ &+ (\nabla U)(\nabla\mu) + f_{st} \end{aligned} \tag{18}$$

The final form of the transport equation (Eq. (17)) must be solved simultaneously with the continuity equation for the incompressible flow (Eq. (16)) and the momentum equation (Eq. (18)), together with the constitutive relations for density and dynamic viscosity (Eq. (13)).

This code is based on the finite volume discretization method. A second upwind discretization scheme is used to consider the stability of solution convergence, and the SIMPLE algorithm is employed for the pressure-velocity coupling. In order to model turbulence, the k-ε turbulence and RSM are selected. The k-ε model is based on a transport equation for turbulent kinetic energy, k, and a transport equation for the turbulent kinetic energy dissipation, ε. An important restriction for applying the k-ε model is that the solution for the system of equations converges to a 'steady-state' result. The standard k- ε model is a two-equation model based on a transport equation for turbulent kinetic energy k as well as a transport equation for the turbulent kinetic energy dissipation ε 0. It could be observed from the results that this

model could not model the secondary flow, especially at the outflow. For this purpose, the RSM is used for modeling the turbulence flow.
The RSM [13] is one of the most complicated turbulence models. Regardless assumptions for the isotropic eddy-viscosity, the RSM closes the Reynolds-averaged Navier-Stokes equations through solving transport equations for the Reynolds Stresses as well as an equation for the dissipation rate. In the other words, seven additional transport equations are supposed to be solved in three dimensions. RSM, due to its consideration of the effects of streamline curvature, swirl, rotation and rapid changes in strain rates, has a greater potential to predict complex flows accurately than one or two-equation models. However, the precision of RSM predictions is still limited by the closure assumptions applied to various terms of the model in the exact transport equations for Reynolds stresses.
According to the operating conditions, simulations of two-phase flow are used. VOF method is utilized to compute the free surface conditions. The convergence criterion determines the procedure that the global residuals would decrease to less than 0.0001 for discretized equations. However, it should be considered that one of the outputs obtained by calculations, such as air ventilation, should converge to a constant value. The boundary conditions considered for this problem are mentioned below:

$$\begin{aligned} &Velocity\ Inlet \rightarrow u_x = u_{Inlet},\ v_y = 0 \\ &I = 5.5,\ Hydraulic\ Diameter = 0.666 \\ &Pressure\ Inlet \rightarrow P = P_{Inlet},\ \frac{\partial \varphi}{\partial x} = 0 \\ &Pressure\ Outlet \rightarrow P = P_{\infty},\ \frac{\partial \varphi}{\partial x} = 0 \\ &Wall \rightarrow u_x = 0,\ v_y = 0 \end{aligned} \quad (19)$$

5. Mesh generation

Hexagonal elements have been used due to their ability to follow the streamlines close to the body, possibility of making them long parallel to the body and thin orthogonal to the body, and eventually, lower need to node points rather than tetrahedral elements. For generating the hexahedral cells, the domain should be divided into five zones. The air ventilation is checked for independence to the cell number as depicted in Fig. 6. It is found out that when the number of cells is more than 4.85 million, the air ventilation changes approximately by 0.64%. The mesh generated for the geometry is displayed in Fig. 7.

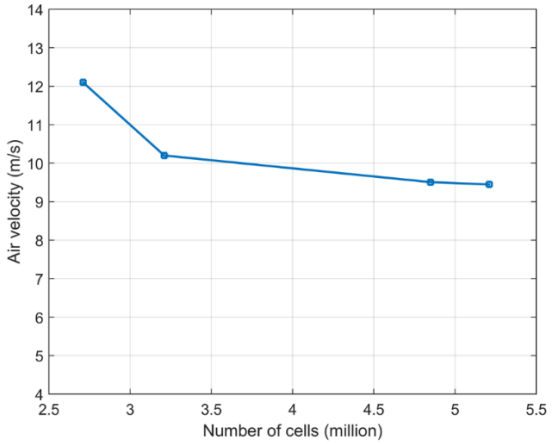

Fig. 6. Air ventilation grid independency.

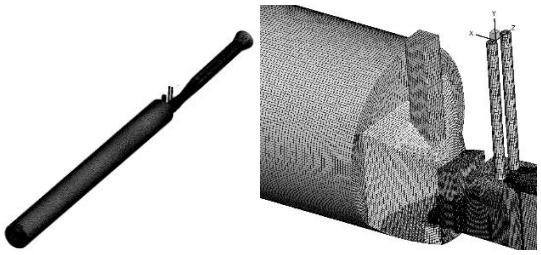

Fig. 7. The mesh generated for the tunnel geometry.

The outcomes achieved from the numerical and experimental analysis include air ventilation and discharge coefficient along the duct. In numerical method, the results obtained from two turbulence models of k-ε and RSM are illustrated in Fig. 8. Regarding the fact that the critical state occurs in a 100 percent opening of the service gate, the analysis is conducted for three states of opening: 50%, 80%, and 100%. The air inflow rate in three states of the opening of 50%, 80%, and 100% is displayed in Fig. 8. It can be seen that the k-ε model exhibits a better capability than RSM.

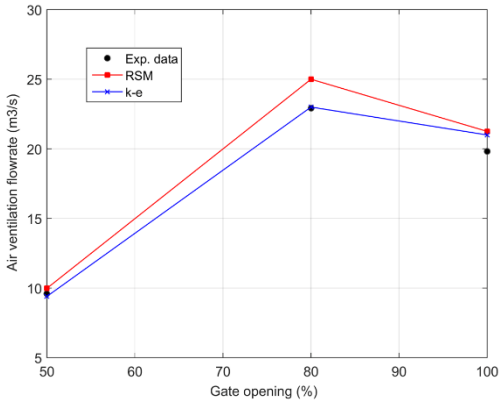

Fig. 8. Comparison between the results obtained by two models, RSM and k-ε, for the air inflow rate in three states.

6. Discharge coefficient investigation

In fluid mechanics, empirical coefficients are used to correct the flow rate calculated from the energy equation. Accordingly, the flow rate coefficient (C_d) determines the ratio of the actual flow rate (Q) to the rate calculated theoretically (Q_t). The flow rate coefficient passing under the valves is defined as follows:

$$C_d = \frac{Q}{Q_t} = \frac{Q}{A\sqrt{2gH}} \tag{20}$$

where A is the cross-section of the valve opening percent and H is the water head which is used in two forms. If the difference between the upstream tank level and the jet axis of the valve outflow is considered, it is represented as the tank head, and if the effective head on the reference pisometer is employed, it is displayed as the reference head. In fact, C_d for the evacuator valve depends on factors including the geometry of the valve and its edge, the geometrical shape of the upstream duct, the flow status and the effective water height. In Fig. 9, the discharge coefficient in different opening percent is displayed. As observed, the k-ε model has better performance in predicting the discharge coefficient. However, by predicting the flow profile, the k-ε method could not accurately show the water flow profile inside the air in the downstream. This could have happened cause of the presence of secondary flows after colliding water to the channel floor. This is intensified at the end of the channel, and the flow modeled by the k-ε method moves to the middle of the channel instead of a side motion. But RSM method has better abilities in protecting the flow profiles due to its additional terms in modeling the turbulent flow. This distinction could be simply observed in Figs. 10-12.

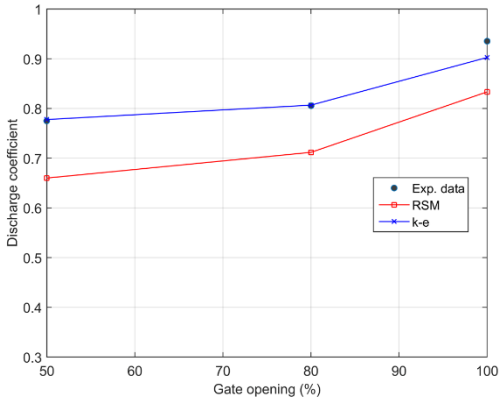

Fig. 9. The discharge coefficient in different Opening percent for different models and experimental data.

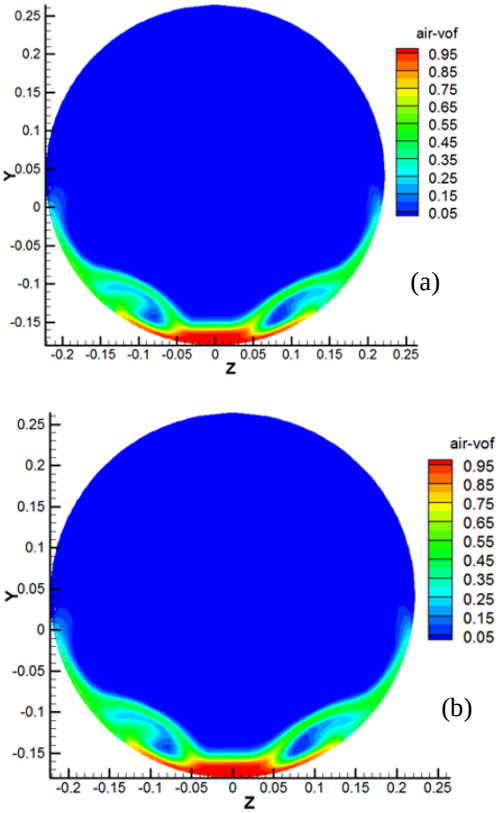

Fig. 10. Contour of volume fraction for water one meter after the valve for an opening of 50%; (a) RSM, and (b) k-ε method.

As shown in Fig. 13, the modeled flow at the outlet moves to the middle of the channel. Regarding the intense reduction of pressure after the gate, the air intake is supplied from both the inside duct after the gate and the outlet of the evacuator. As experimental results demonstrate the air intake from the outlet end of the open flow, the numerical results for both methods are also verified the same fact. In Fig. 14, the velocity field is observed as the reverse motion of the water flow for air in the drawn streamlines.

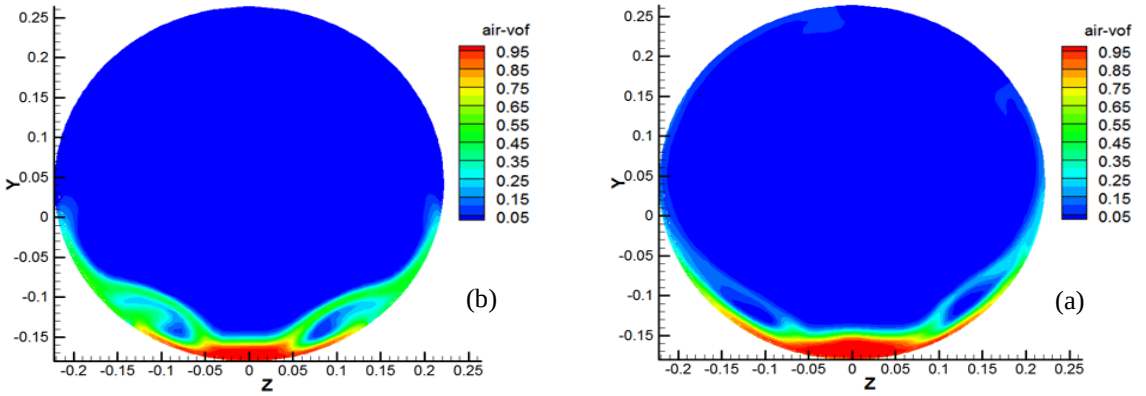

Fig. 11. Contour of volume fraction for water two meters after the valve for an opening of 50%; (a) RSM, and (b) k-ε method.

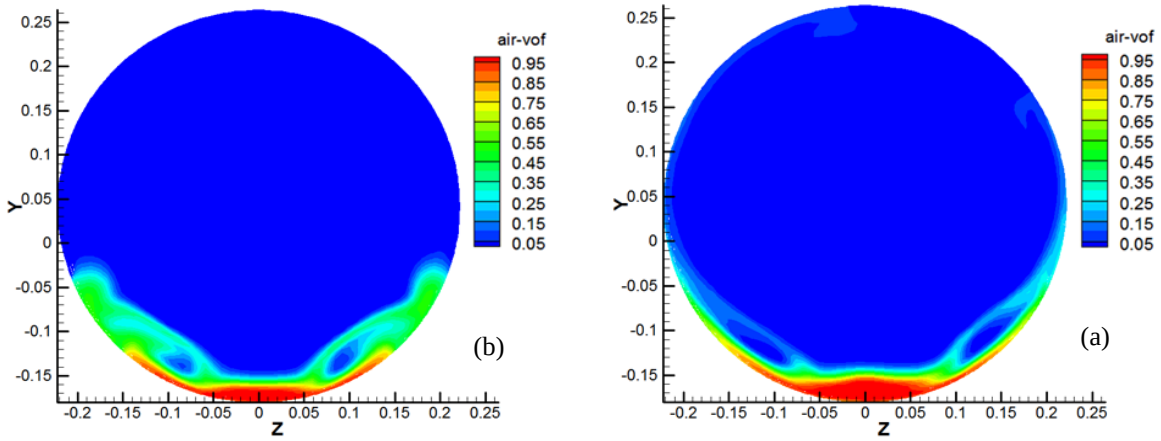

Fig. 12. Contour of volume fraction for water three meters after the valve for an opening of 50%; (a) RSM, and (b) k-ε method.

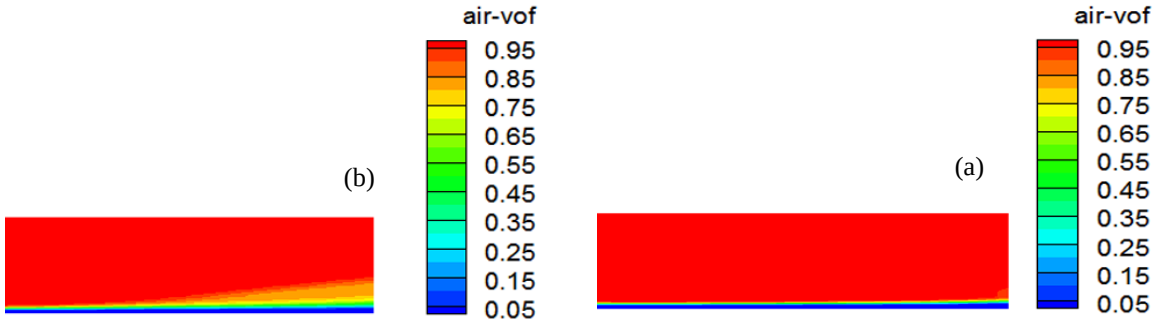

Fig. 13. Contour of volume fraction for outflow water for an opening of 50%, (a) RSM, (b) k-ε method.

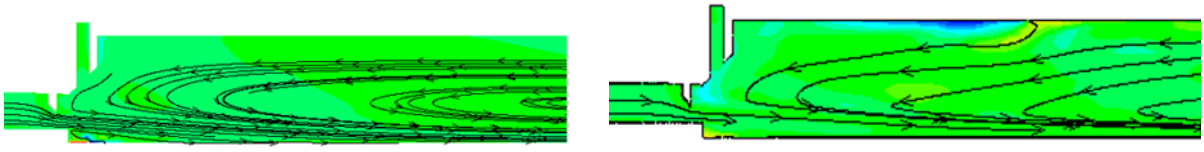

(b) (a)

Fig. 14. The streamlines after the gate in RSM (a) and in k-ε model (b).

7. Conclusions

In this research, the flow of air in a gated tunnel is simulated. The numerical model includes solving the Navier-Stokes equation in which the VOF model is used to simulate complicated air-water flow. In order to model turbulence flow, the RSM and k-ε models are employed. Comparing the numerical results obtained from the two methods together with the experimental results indicates that the RSM model has higher accuracy. The RSM method could better predict the flow profiles due to its additional terms in modeling the turbulent flow. However, the RSM is more expensive and time-consuming because of its solution of additional equations, and a lower under-relaxation factor is supposed to be used for results convergence, and this could increase the computation time as well. By comparing the results for various openings, it can be indicated that the highest velocity of the airflow is 17.7 m/sec for an opening of 80%. It was also observed that the discharge coefficient increases by a rise in the opening of the valve which is known to be due to the pressure drop resulted from the valve.

Reference

[1] A. Kalinske, and J. M. Robertson, "Closed conduit flow", *ASCE Transactions*, Vol. 108, pp. 1435-1447, (1943).

[2] H. R. Sharma, "Air entrainment in high head gated conduits", *Journal of Hydraulics Division, ASCE,* Vol. 102, No. 11, pp. 1629-1646, (1976).

[3] J. Speerli and P. U. Volkart, "Air entrainment in bottom outlet tailrace tunnels", *Proceedings of the 27th IAHR Congress*, San Francisco, Theme D, pp. 613-618 (1997).

[4] M. J. Kenn and A. D. Garrod, "Cavitation damage and the Tarbela tunnel collapse of 1974", *Proc. Institution Civil Engineers*, Vol. 70, No. 1, pp. 65- 89 (1981).

[5] J. Speerli, W. H. Hager, "Air-water flow in bottom outlets", Canadian Journal of Civil Engineering, Vol. 27, pp. 454-462 (2000).

[6] K. H. Safavi and A. R. Zarrati, J. Attari, "Experimental study of air demand in high head gated tunnels", *Journal of Water Management*, Vol. 161, (2008).

[7] B. Dargahi, "Flow characteristics of bottom outlets with moving gates", *Journal of Hydraulic Research*, Vol. 48, No. 4, pp. 476-482, (2010).

[8] J. Yazdi and A. R. Zarrati, "An algorithm for calculating air demand in gated tunnels using a 3D numerical model", *Journal of Hydro-environment Research*, Vol. 5, pp. 3-11, (2011).

[9] R. Kolachian, A. Abbaspourand F. Salmasi, "Aeration in Bottom Outlet Conduits of Dams for Prevention of Cavitation", *Journal of Civil Engineering and Urbanism*, Vol. 2, No. 5, pp. 196-201, (2012).

[10] A. Kiczko, J. Kubrak, E. Kubrak, "Experimental and numerical investigation of non-submerged flow under a sluice gate", *Annals of Warsaw University of Life Sciences*, Vol. 47, No. 3, pp. 187-201, (2015).

[11] S. Y. Kumcu, "Investigation of flow over spillway modeling and comparison between experimental data and CFD analysis", *KSCE Journal of Civil Engineering*, Vol. 21, No. 3, pp. 994-1003, (2017).

[12] N. M. Nouri, M. Moghimi, S. M. Mirsaeedi, "Numerical Simulation of unsteady cavitating flow over a disk", *Journal of Mechanical Engineering, part C*, Vol. 224, pp. 1245-1253, (2009).

[13] B. E. Launder and D. B. Spalding. "*Lectures in Mathematical Models of Turbulence*", Academic Press, London, England, (1972).

How to cite this paper:

M. Moghimi, M. Kalantar, E. Molavi, " Experimental and numerical investigation of bottom outlet hydraulic model" *Journal of Computational and Applied Research in Mechanical Engineering*, Vol. 8, No. 2, pp. 153-164, (2018).

DOI: 10.22061/jcarme.2018.1627.1140

URL: http://jcarme.sru.ac.ir/?_action=showPDF&article=827